IL NUOVO CIMENTO Vol. 36 C, N. 4 Luglio-Agosto 2013
DOI 10.1393/ncc/i2013-11550-2

Communications: SIF Congress 2012

Amperometric detection of quantal catecholamine secretion from individual cells by an ion beam microfabricated single crystalline diamond biosensor

F. Picollo(*)

Physics Department - University of Torino, Torino, Italy
NIS Centre of Excellence - University of Torino, Torino, Italy
INFN, Sezione di. Torino, Torino, Italy and
Consorzio Nazionale Interuniversitario per le Scienze Fisiche della Materia (CNISM)
Sezione di Torino, Torino, Italy

ricevuto il 31 Dicembre 2012

Summary. — It is shown that buried graphitic channels fabricated in monocrystalline diamond by selective damage induced by focused MeV ions, can be considered an effective alternative to the commonly used carbon-fibers to detect the catecholamine release from cells as individual secretory granules discharge their contents during the process of quantal exocytosis. Quantal secretory responses have been measured from stimulated chromaffin cells, which were positioned on the graphitic microelectrode, polarized to +800 mV. Sequences of amperometric spikes started after cell stimulation with the KCl solution, with amplitudes well above the background noise within the range of 8–180 pA and comparable with signals obtained by conventional carbon fiber electrodes.

PACS 85.40.Hp – Lithography, masks and pattern transfer.
PACS 81.05.uj – Diamond/nanocarbon composites.
PACS 87.85.D- – Applied neuroscience.

1. – Introduction

Following our previous studies on the formation of conductive graphitic microchannels in single-crystal diamond by means of direct lithography with a scanning ion microbeam [1-5], it is reported on the fabrication and preliminary testing of a cellular biosensor with the above-mentioned technique.

The so-called "Lab-on-a-chip" devices are highly demanded in modern biotechnology to cultivate living cells for long periods while inducing and revealing a broad range of electrical biosignals, such as the quantal release of bioactive molecules from neurons and neuroendocrine cells.

(*) E-mail: picollo@to.infn.it

An integrated diamond-based device can effectively address many open issues in the existing cell-sensing research which to different extents are not met by conventional biomaterials (silicon [6], gold [7, 8], platinum [9, 10], indium-doped tin oxide [11-13], diamond-like carbon [14-16], carbon nanotubes [17] and conductive polymers [18]), such as robustness and reproducibility in performance over repeated biosensing cycles, biocompatibility and long-term stability for *in vivo* measurements and high transparency for optical interfacing.

Here it is reported on the MeV-ion-beam fabrication process of a diamond cellular substrate with graphitic electrodes, and on the results of its preliminary characterization for the detection of exocytosis activity from chromaffin cells. The results obtained with the diamond biosensor are also compared with conventional electrodes such as carbon microfibers.

Carbon fiber microelectrodes (CFEs) are employed since few decades to detect the exocytotic activity of single excitable cells with amperometric techniques and provide significant information on key mechanisms such as the formation of the fusion pore and the kinetics of single secretory events in real time [19-22].

2. – Device microfabrication

In the present work an artificial single-crystal diamond sample produced by Sumitomo Electric by means of "high pressure high temperature" (HPHT) technique was employed. Sample size is $3 \times 3 \times 1.5\,\mathrm{mm}^3$ and the crystal is classified as type Ib, *i.e.* its substitutional nitrogen concentration is comprised between 10 and 100 ppm.

The sample was implanted at the ion microbeam line of the AN2000 accelerator of the Legnaro National Laboratories with a scanning beam of 1.8 MeV He^+ ions at typical fluences of $\sim 5 \cdot 10^{17}\,\mathrm{cm}^{-2}$. Ion beam size was $10\,\mu$m, while beam currents were comprised between 5 nA and 8 nA, thus ensuring typical implantation times of 50 minutes. The sample was metal-coated to avoid surface charging and fluence was accurately monitored with an electrometer connected to the sample chamber, which is electrically insulated from the rest of the beamline, thus acting effectively as a Faraday cup.

As reported in previous works [1-5], high-fluence MeV ion implantation determines the formation of a sub-superficial amorphized layer in correspondence of the ion end-of-range. In the present work, ion implantation led to the formation of a ~ 300 nm thick amorphous layer at a depth of $3.2\,\mu$m below the sample surface. The employment of variable-thickness masks defined on the sample surface by means of non-contact metal evaporation allowed the gradual modulation of the penetration depth of the MeV ions, thus ensuring the emergence of the buried layers at the sample surface at specific locations, as schematically shown in fig. 1.

After ion implantation, the sample was annealed in vacuum at a temperature of 1100 °C for 2 hours. The process resulted in the conversion of the amorphized layer to a graphitic phase, while the surrounding regions which were damaged below a critical threshold reconverted to the pristine diamond form. One of the electrically conductive graphitic microchannels was subsequently connected to the acquisition electronic chain by means of a standard metal contact, while the other emerging end defined the location at the sample surface where biochemical sensing was performed, as schematically shown in fig. 2.

It is worth underlying that the micro-electrode is employed to monitor the activity of a living cell, which during the *in vitro* measurements is immersed in a physiological solution: for this reason buried connections embedded in the insulating diamond matrix

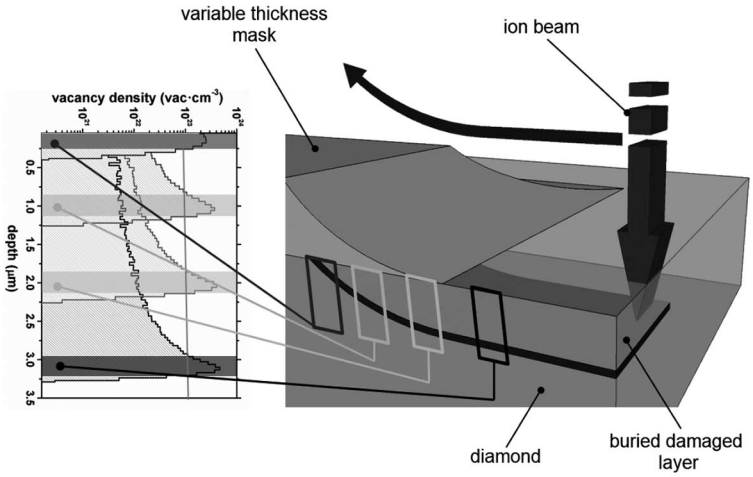

Fig. 1. – Schematics of the variable-thickness process allowing the definition of the buried amorphous layer at variable depth.

are demanded, and the metal macro-contacts are shielded with a biocompatible insulating mask in "sylgard" polymer.

Before proceeding with the functional tests reported in the following section, two-points electrical characterization (see fig. 3) was performed to check that i) the buried electrical channels get in electrical contact with the sample surface at their endpoints and ii) the electrical resistivity of the microchannels is compatible with that of polycrystalline graphite (*i.e.* $\sim 3 \cdot 10^{-3}\,\Omega\,\mathrm{cm}$).

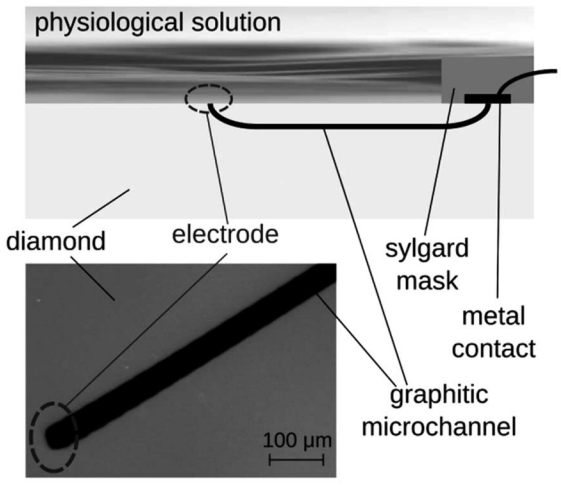

Fig. 2. – Top: Lateral view schematics of the diamond device incorporating the graphitic microchannel. Bottom: top view micrograph of the microelectrode at the endpoint of the graphitic microchannel.

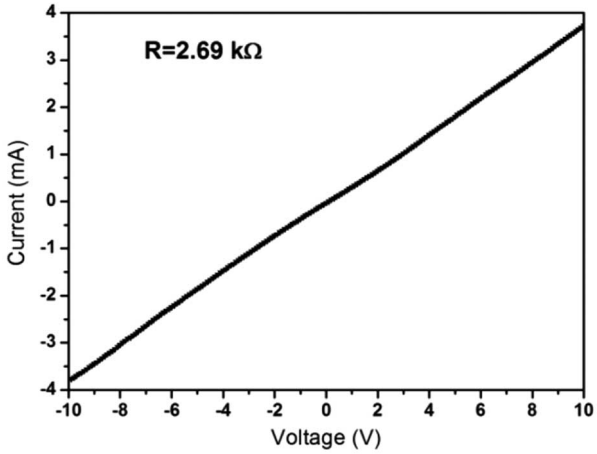

Fig. 3. – Current-voltage characteristic of buried conductive channel.

3. – Exocytosis detection from chromaffin cells

The exocytosis of neurotransmitters is the biological process taken under exam and has been studied by means of detection of adrenaline secretion from the chromaffin cells with the diamond-base biosensor.

Those cells are located into the medulla part of the adrenal gland, are characterized by the presence inside them of granules. Those granules have size ranged from 150 to 350 nm and contain high concentration of catecholamines as adrenaline and noradrenaline (0.5–1 M).

Stress conditions induce the medulla gland to secrete catecholamines in order to stimulate target organs (*i.e.* heart frequency increase, bronchus dilatation, etc.).

The chromaffin cells can be studied as model for neuron secretion since those are electrically excitable cells, have an exocytic apparatus analogous of neurons one and secrete the same family of neurotransmitters (catecholamines). Moreover, chromaffin cells have large dimension (10–20 μm) then neuron's synapses and are easily cultivable and isolable.

The responsiveness of the device towards catecholamines (adrenaline, noradrenaline) was preliminarily tested by means of cyclic voltammetry measurements.

As shown in fig. 4, when immersed in a saline solution containing 10 mM adrenaline, the device can detect the oxidation of the adrenaline molecules at the electrode when the voltage reaches +0.8 V, as opposed to the case when a standard saline solution (in mM: 128 NaCl, 2 $MgCl_2$, 10 glucose, 10 HEPES, 10 $CaCl_2$, 4 KCl) is employed.

Following these preliminary tests, the device was tested by positioning an isolated chromaffin cell in correspondence of the active region, while keeping the whole system in physiological solution.

The micro-electrode was polarized at the fixed voltage corresponding to the oxidation of the adrenaline (*i.e.* 0.8 V, as reported in fig. 4), in order to detect, via amperometry, the quantal release occurring during exocytosis. Perfusion of KCl-enriched solution was employed to stimulate the adrenaline secretion from chromaffin cells. As reported in fig. 5, the device is able to detect with high signal-to-noise ratio the amperometric spikes of 3–22 pA corresponding to the quantal release of catecholamines.

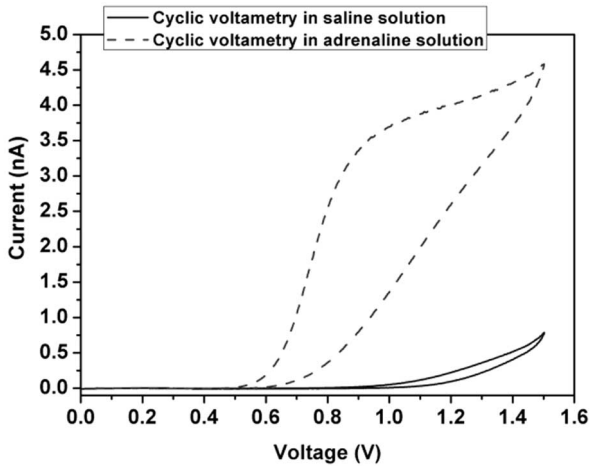

Fig. 4. – Cyclic voltammetry tests on saline and adrenaline-containing solutions. The adrenaline oxidation feature at $V = 0.8\,\mathrm{V}$ is clearly visible.

Systematic data analysis of amperometric spikes was performed by means of "Igor" macros, as previously described in [23]. The amplitude of most visible amperometric spikes were well above the background noise (5 pA peak-to-peak) and varied from 8 pA to 180 pA. The background noise of graphitic microelectrode has the same amplitude of CFE one (data not reported).

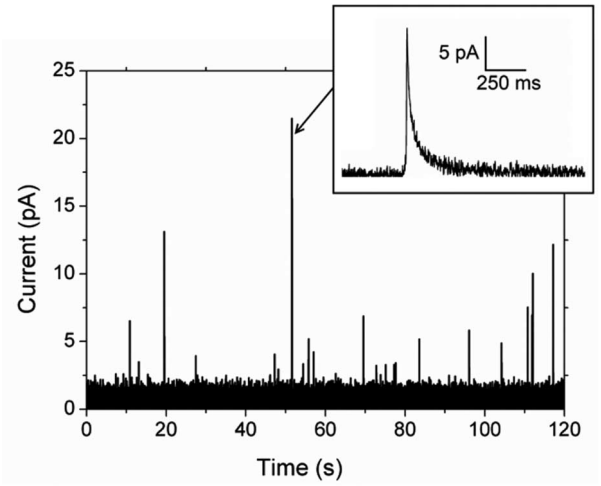

Fig. 5. – Time course of amperometric signals detected from a single chromaffin cell located in correspondence of the active region of the device: the spikes (zoom in the inset) correspond to single exocytotic events.

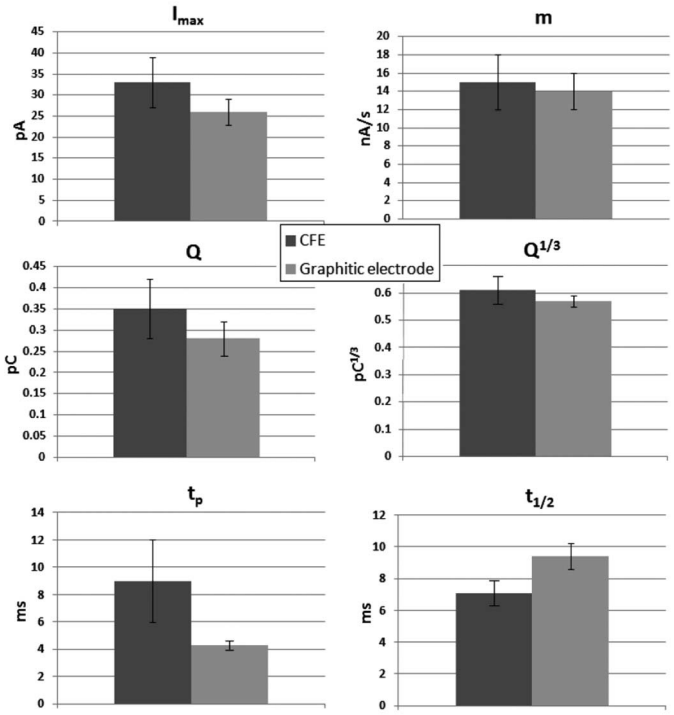

Fig. 6. – Histograms of characteristic parameters of spikes. Each graph shows the comparison of the results obtained with carbon fibre electrode and micrographitic channels. The represented spikes's parameters are: $I_{\max}$ maximum of current amplitude, m slope of gradient, Q integral of the peak (total charge measured), $Q^{1/3}$ cube root of Q, t_p time needed to reach the maximum of the peak, $t_{1/2}$ full width at half maximum of the peak.

Information of exocytosis process are obtained by the characteristic parameters of amperometric spikes.

The parameters analyzed for our measurements are summarized below and represented in the fig. 6:

- $I_{\max}$: maximum of current amplitude due to adrenaline oxidation;
- Q: integral of the peak which is the total charge of one granule;
- $Q^{1/3}$: cube root of Q, this parameter is proportional to the granules' radius;
- m: slope of gradient gives information concerning the evolution of fusion pore (aperture that allows the release of neurotransmitters from the granule to the outside of the cell membrane);
- t_p: time needed to reach the maximum of the peak, it indicates the time in which the granule releases all the adrenaline;
- $t_{1/2}$: full width at half maximum of the peak.

As indicated in fig. 6, amperometric spikes recorded by the graphitic microelectrode ($n = 94$ spikes) are comparable with signals obtained by conventional CFEs. This is particularly clear comparing the more interesting biological parameters as the mean current amplitude (26±4 pA and 33±6 pA values measured with graphitic microelectrode

and CFE, respectively) and the mean collected charge (0.28 ± 0.04 pC *versus* 0.35 ± 0.07 pC measured with graphitic microelectrode and CFE, respectively). The discrepancy observed for the t_p parameter is probably due to difference on cells' stimulation (*i.e.* non-equal volumes of perfused KCl-enriched solution) that justify also a large error bar for CFE measurement.

4. – Conclusions

Buried conductive micro-channels were fabricated by means of direct writing with a scanning MeV ion-beam, taking advantage of the possibility offered by a high-energy ion probe to locally amorphize and subsequently graphitize the diamond structure. *In vitro* detection of quantal neurotransmitter release from single excitable cells kept in a physiological solution was performed.

It is worth noting that the performance (amperometric sensitivity, signal-to-noise ratio, time resolution) of the prototypical diamond-based device presented in this work compare well not only with standard CFEs (see fig. 6), but also with other well developed technologies at the state of the art, such as devices based on indium tin oxide (ITO) conductive glass [12, 13, 17], noble metals (Au, Pt, ...) [8, 15] and boron-doped nanocrystalline diamond (B:NCD) [23]. In comparison with devices based on CFEs, ITO and noble metals, our device offers the advantages of an all-carbon architecture which is advantageous in terms of chemical stability and biocompatibility, and a broader electrochemical window. In conclusion, these results open promising perspectives for the realization of all-carbon multielectrode miniaturized devices in artificial diamond (a material which is becoming available with increasing crystal quality at ever-decreasing costs [24, 25] in which full advantage of the robustness, chemical stability, biocompatibility and transparency can be exploited to obtain multiparametric signals detection from cell networks. This approach has the potential to drastically accelerate data collection from large ensembles of cells, leaves the experimental sample under physiological conditions. In addition, it is non-invasive and allows repeated measurements over time. Furthermore, geometry and transparency of the structures allows multi-techniques measurements, since other probes (*i.e.* patch-clamp pipettes) can be easily adapted.

* * *

This work was supported by: "FIRB - Futuro in Ricerca 2010" project (CUP code: D11J11000450001), funded by the Italian Ministry of Education, University and Research (MIUR); "Micro.Di.Bi." project, funded by the "BioPMed" scientific pole of Regione Piemonte; "Linea 1A ORTO11RRT5" projects of the University of Torino, funded by "Compagnia di San Paolo".

REFERENCES

[1] Olivero P., Amato G., Bellotti F., Budnyk O., Colombo E., Jakšić M., Lo Giudice A., Manfredotti C., Pastuović Ž., Picollo F., Skukan V., Vannoni M. and Vittone E., *Diamond Relat. Mater.*, **18** (2009) 870.

[2] Olivero P., Amato G., Bellotti F., Borini V, Lo Giudice A., Picollo F. and Vittone E., *Eur. Phys. J. B*, **75 (2)** (2010) 127.

[3] Picollo F., Olivero P., Bellotti F., Pastuović Ž., Skukan N., Lo Giudice A., Amato G., Jakšić M. and Vittone E., *Diamond Relat. Mater.*, **19** (2010) 466.

[4] Olivero P., Forneris J., Jakšić M., Pastuović Ž., Picollo F., Skukan N. and Vittone E., *Nucl. Instrum. Methods B*, **269** (2011) 2340.
[5] Picollo F., Gatto Monticone D., Olivero P., Fairchild B. A., Rubanov S., Prawer S. and Vittone E., *New J. Phys.*, **14** (2012) 053011.
[6] Chen P., Xu B., Tokranova N. B., Feng X., Castracane J. and Gillis K. D., *Anal. Chem.*, **75** (2003) 518.
[7] Cui H. F., Ye J. S., Chen Y., Chong S. C. and Sheu F. S., *Anal. Chem.*, **78** (2006) 6347.
[8] Dittami G. M. and Rabbitt R. D., *Lab Chip*, **10** (2010) 30.
[9] Dias A. F., Dernick G., Valero V., Yong M. G., James C. D., Craighead H. G. and Lindau M., *Nanotechnology*, **13** (2002) 285.
[10] Hafez I., Kisler K., Berberian K., Dernick G., Valero V., Yong M. G., Craighead H. G. and Lindau M., *Proc. Natl. Acad. Sci. U.S.A.*, **102** (2005) 13879.
[11] Sun X. and Gillis K. D., *Anal. Chem.*, **78** (2006) 2521.
[12] Chen X., Gao Y., Hossain M., Gangopadhyay S. and Gillis K. D., *Lab Chip*, **8** (2008) 161.
[13] Meunier A., Fulcrand R., Darchen F., Guille Collignon M., Lemaître F. and Amatore C., *Biophys. Chem.*, **162** (2012) 14.
[14] Parpura V., *Anal. Chem.*, **77** (2005) 681.
[15] Gao Y., Chen X., Gupta S., Gillis K. D. and Gangopdhyay S., *Biomed. Microdevices*, **10** (2008) 623.
[16] Sen A., Barizuddin S., Hossain M., Polo-Parada L., Gillis K. D. and Gangopadhyay S., *Biomaterials*, **30** (2009) 1604.
[17] Shi B. X., Wang Y., Zhang K., Lam T. L. and Chan H. L. W., *Biosens. Bioelectron.*, **26** (2011) 2917.
[18] Larsen S. T. and Taboryski R., *Analyst*, **137** (2012) 5057.
[19] Chow R. H., von Rüden L. and Neher E., *Nature*, **356** (1992) 60.
[20] Travis E. R. and Wightman R. M., *Annu. Rev. Biophys. Biomol. Struct.*, **27** (1998) 77.
[21] Wightman R. M., *Science*, **311** (2006) 1570.
[22] Amatore C., Arbault S., Guille M. and Lemaître F., *Chem. Rev.*, **108** (2008) 2585.
[23] Carabelli V., Gosso S., Marcantoni A., Xu Y., Colombo E., Gao Z., Vittone E., Kohn E., Pasquarelli A. and Carbone E., *Biosens. Bioelectr.*, **26** (2010) 92.
[24] Butler J. E., Mankelevich Y. A., Cheesman A., Ma J. and Ashfold M. N. R., *J. Phys. Cond. Matter*, **21** (2009) 364201.
[25] Teraji T., *Phys. Status Solid. A*, **203** (2006) 3324.